

Influence of Oxygen Content on the Activation Energy for Oxygen Ordering in $\text{Tl}_2\text{Ba}_2\text{CuO}_{6+\delta}$

C.W. Looney^a, J.E. Kline^b, F. Mascarenhas^b, J.S. Schilling^b, and A.M. Hermann^c

^aDept. of Physics, Merrimack College, 315 Turnpike Street, North Andover, MA 01845

^bDept. of Physics, Washington University, C.B. 1105, One Brookings Drive, St. Louis, MO 63130

^cDept. of Physics, University of Colorado, C.B. 390, Boulder, CO 80309

August 25, 2000

Abstract

The activation energies E_A for both low temperature (LT) (< 120 K) and high temperature (HT) (> 200 K) oxygen ordering processes in $\text{Tl}_2\text{Ba}_2\text{CuO}_{6+\delta}$ single crystals have been estimated from the time dependence of T_c following the release of high pressure (0.6 GPa) at low temperatures. The crystals studied have T_c values of 29 K (strongly overdoped), 40 K (moderately overdoped), and 70 K (slightly overdoped). For both HT and LT processes E_A is clearly largest for the 29 K sample; for the HT process E_A appears to be slightly smaller for the 40 K sample than for the 70 K sample, but approximately equal for the LT process. Possible mechanisms are discussed.

1 Introduction

It is well known that T_c exhibits a sensitive dependence on oxygen content in the high- T_c oxides. In underdoped $\text{YBa}_2\text{Cu}_3\text{O}_{6+x}$ (Y-123), augmenting the oxygen content in the Cu-O chains from $x \approx 0.3$ to 0.9 causes T_c to increase from 0 K to over 90 K [1], whereas in overdoped $\text{Tl}_2\text{Ba}_2\text{CuO}_{6+\delta}$ (Tl-2201) T_c decreases from ~ 90 K to 0 K upon the addition of $\delta \approx 0.15$ units of oxygen to an interstitial site within the Tl_2O_2 double layer [2]. In addition, the transition temperature in the high- T_c oxides can depend strongly on the *configuration* of oxygen defects within the lattice, even at fixed oxygen concentration. Quenching underoxygenated Y-123 from 500°C to 77 K freezes in disorder and suppresses T_c by more than 20 K; subsequent annealing at room temperature causes T_c to creep back up toward its initial value as the oxygen defects relax towards a higher degree of order at this lower temperature [3]. This increase in T_c results from an increase in the concentration of hole carriers in the CuO_2 plane [4].

The degree of order in the oxygen sublattice is also enhanced by the application of high pressures. In a series of hydrostatic pressure experiments to 0.8 GPa on polycrystalline $\text{Tl}_2\text{Ba}_2\text{CuO}_{6+\delta}$ (Tl-2201) with varying oxygen content, Sieburger and Schilling [5] made the surprising observation that the pressure derivative $(dT_c/dP)_{\text{RT}}$ for pressure changes at room temperature (RT) may differ substantially from the rate $(dT_c/dP)_{\text{LT}}$ for pressure changes at low temperatures (LT) below ~ 55 K. Furthermore, they found that both the LT and RT pressure derivatives depend sensitively on the concentration of interstitial oxygen δ ; this fact, combined with the significant mobility of oxygen in many high- T_c oxides, led them to propose that pressure-induced ordering within the interstitial oxygen sublattice is responsible for the strong dependence of dT_c/dP on temperature. Presumably, the interstitial oxygen can move around and order in response to pressure changes at RT, thereby altering the number of holes in the conduction layer, whereas at LT these oxygen anions are frozen in place. Since the initial work on Tl-2201, related pressure-induced effects have been observed in a number of additional high- T_c materials [6, 7, 8, 9, 10, 11, 12, 13].

The dramatic influence that pressure-induced oxygen ordering can have on the pressure dependence $T_c(P)$ is well illustrated by the diamond anvil cell work of Looney *et al.* [14] on Tl-2201 shown in Fig. 1. The application of pressures as high as 5.5 GPa at RT suppresses T_c from its initial ambient pressure value of 40 K down to nearly 10 K. Following the release of pressure at 6 K, T_c does not return to its initial ambient pressure value but instead increases only slightly. If the sample is now annealed for 1 hour at successively higher temperatures up to 300 K, T_c is seen to relax back to its initial value in a *two-step* fashion, indicating the presence of both LT and HT relaxation processes with activation energies of ~ 0.25 eV and ~ 0.72 , respectively. Only HT processes have been observed in all other high- T_c materials studied to date. It has been proposed [15] that the LT relaxation in Tl-2201 results from the coordinated rearrangement of interstitial oxygen defects in the Tl_2O_2 double layer between degenerate sites *within* the unit cell, whereas the HT process originates from the migration of the interstitial oxygen from one unit cell to another. This picture has received some support from a recent comparison of the measured activation volume for Tl-2201 with a hard-sphere model calculation [16].

It would clearly be of interest to better characterize both LT and HT relaxation processes in superconducting Tl-2201 by systematically determining their relative magnitudes and associated activation energies E_A over the entire range of oxygen content. In the present paper we present the results of recent experiments which probe pressure-induced oxygen ordering effects in single crystalline Tl-2201 samples with T_c values in the range 15 K to 70 K. These data are compared with the results of previous studies on both single-crystalline [15, 16] and polycrystalline [5] Tl-2201 samples, in particular a 40 K crystal. All samples exhibit the two-step relaxation behavior characteristic for Tl-2201. E_A for both LT and HT processes is found to be largest for the most heavily oxygen-doped Tl-2201 samples, in contrast to the systematics for the Y-123 system [6]; for the HT process, E_A appears to be slightly

smaller for the 40 K than for the 70 K crystal.

2 Experimental

The Tl-2201 single crystals used in the present and previous studies were synthesized at the University of Colorado; the details of the synthesis procedure are given elsewhere [15]. The ambient pressure T_c values of the crystals studied here were ~ 70 K, 29 K, and 15 K with crystal dimensions $500 \times 300 \times 20 \mu\text{m}^3$, $580 \times 330 \times 20 \mu\text{m}^3$ and, $700 \times 500 \times 60 \mu\text{m}^3$, respectively. The high pressure studies were carried out at Washington University using a helium gas high-pressure system which allows the pressure to be changed at any temperature above the melting curve T_m of helium (for example, $T_m \simeq 13.8$ K at 0.1 GPa and $T_m \simeq 52.4$ K at 0.8 GPa). Superconducting transition temperatures were determined from the real part of the ac susceptibility at 1.13 Oe rms magnetic field at 507 Hz. To allow the most meaningful comparison, the 70 K and 29 K crystals were measured together in the same pressure cell. As seen in Fig. 2, the widely differing values of T_c for these two crystals at ambient pressure prevented any mutual interference in the ac susceptibility measurement. Both samples exhibited full shielding with 10-90 transition widths of less than 1.5 K. By superposing the transition curves, shifts in T_c under pressure could be determined with a typical uncertainty of ~ 30 mK [17]. The experimental technique is described in detail elsewhere [18].

3 Results of Experiment

3.1 The Pressure Dependence of T_c

In Fig. 3 are shown the present results for the pressure dependence of T_c on the two simultaneously measured Tl-2201 crystals described above. Following the initial determination of $T_c(1 \text{ bar}) = 70.20$ K and 28.50 K for each sample (point 1), the samples were warmed to RT (~ 300 K) where a pressure of 0.17 GPa was applied over a 5 minute period. After a one hour RT annealing period at this pressure, the samples were cooled in 2 hours to low temperature to measure T_c (point 2). The samples were then warmed back up to RT, and the aforementioned measurement cycle (pressure increase at RT, one hour anneal at RT, cooldown to measure T_c) was repeated for pressures of 0.47 GPa and 0.72 GPa, yielding points 3 and 4. Note that the pressure decreases somewhat upon cooling due to the contraction of the helium pressure medium. From these data, using the average values of the pressure, we estimate $(dT_c/dP)_{\text{RT}} \simeq -(1.6 \pm 0.3)$ K/GPa for the 29 K sample and $(dT_c/dP)_{\text{RT}} \simeq -(3.9 \pm 0.6)$ K/GPa for the 70 K sample; both values are considerably less in magnitude than that -8.9 K/GPa observed for a single crystalline Tl-2201 sample with $T_c(1 \text{ bar}) \simeq 40$ K [15]. This trend, that $(dT_c/dP)_{\text{RT}}$ takes on its maximum

magnitude for Tl-2201 samples with T_c values near 40 K, is in qualitative agreement with previous studies on polycrystalline Tl-2201 [5].

Next, the pressure was fully released over a period of 7 minutes as the temperature slowly decreased from 44 K to 34 K. The transition temperature for the 29 K sample was then immediately remeasured (point 5) and found to remain constant within the experimental uncertainty of 30 mK, i.e. $(dT_c/dP)_{LT} \simeq 0$ K/GPa. This result illustrates the dramatic dependence of dT_c/dP on the *temperature* at which the pressure is changed, a point emphasized above for the 40 K crystal (Fig. 1). A detailed comparison of present and previous results will be given later. The transition temperature of the 70 K sample was not remeasured immediately after the release of pressure at low temperatures as this would have interfered with our search for relaxation effects below 70 K in the 29 K sample, as discussed in detail in the next paragraph.

3.2 Relaxation in T_c versus Temperature (series 1)

Following the release of pressure at LT and the remeasurement of T_c for the 29 K sample, the samples were annealed for one hour periods at successively higher temperatures, a remeasurement of T_c following each anneal. In Fig. 4 the relaxation in T_c is mapped out as a function of increasing annealing temperature. In contrast to the 40 K sample, where relaxation in T_c is observed at temperatures as low as 15 K, no relaxation is observed for the 29 K sample until the annealing temperature is raised above 64.5 K; a similar result was obtained for a 23 K sample [15]. Note that we did *not* determine T_c for the 70 K sample until the annealing temperature reached 64.5 K in order to avoid “annealing out” possible LT relaxation effects in the co-measured 29 K sample below this temperature. After a one hour anneal at room temperature (~ 297 K), the T_c values of both samples relaxed back to within 30 mK of their initial ambient pressure values; further annealing at RT for an additional 6 hours caused only minimal further increases in T_c (15 mK for the 29 K sample and 50 mK for the 70 K sample). From Fig. 4 it is clear that both samples exhibit distinct LT and HT ordering processes separated by a clearly defined “plateau” region.

A visual inspection of Figs. 1, 4(a), and 4(b), reveals that the temperature ranges (and thus the activation energies) for both the LT and HT relaxation processes are higher for the 29 K sample than for the other two. For example, the LT relaxation in the 40 K and 70 K samples would be nearly exhausted by a one-hour anneal at 100 K, while the LT relaxation in the 29 K sample would still have a considerable way to proceed. Similarly, a one hour anneal at 275 K would suffice to exhaust the HT process in the 40 K and 70 K samples, while $T_{\text{anneal}} \approx 300$ K would be necessary to fully relax the HT process in the 29 K sample. We thus anticipate that the activation energy for the 29 K sample will be particularly large. A further discussion of the dependence of the activation energies on oxygen concentration will follow the presentation of the 2nd measurement series.

In Figs. 1, 4(a), and 4(b) it is seen that the relative importance of LT and HT relaxation varies sensitively with the initial value of T_c (or, equivalently, with the concentration of interstitial oxygen) in Tl-2201. In the 40 K sample (Fig.1), the LT ordering process is dominant, accounting for over two-thirds of the total observed relaxation. On the other hand, the HT ordering process dominates for the 29 K sample and the 23 K sample (Ref. [15]). In the 70 K sample, it appears that the HT process is somewhat more important than the LT process, although it should be pointed out that there could be a considerable amount of “hidden” LT relaxation that occurred at temperatures below 70 K, before T_c could be measured. We will postpone a further discussion of these issues until after the results of a second measurement series on these two samples have been presented in the next subsection.

In Fig. 5 we show the partial relaxation data for a 15 K crystal of Tl-2201 which also exhibits the two-step recovery in the LT and HT relaxation upon pressure release from 0.6 GPa at 55 K [19]. Unfortunately, the data set is not sufficient to clearly define the onset temperatures for either the LT or HT relaxation processes, although the data resemble those for the 29 K sample.

3.3 Relaxation in T_c versus Time (series 2)

Whereas in the first measurement series a good qualitative overview of the relaxation behavior in T_c was obtained over a wide temperature range, in the second measurement series we would like to study the LT and HT relaxation behavior more quantitatively and determine the activation energies by annealing at a fixed temperature and measuring how T_c changes with time.

In the second series a pressure of 0.72 GPa was applied at 298 K and maintained for $1\frac{1}{2}$ hours before cooling both 70 K and 29 K samples to LT (~ 50 K) over a two hour period. The pressure was then released [20] in ~ 7 minutes while the temperature was held at 51.5 ± 0.5 K, after which T_c was measured for both samples. Next, the samples were annealed for increasing periods of time at 82 K, with a remeasurement of both transitions after each anneal up to a total time of 118 hours, yielding the data in Figs. 6(a) and 6(c), respectively. The samples were then annealed at their respective plateau temperatures (149 K for the 29 K sample and 121 K for the 70 K sample, as seen in Fig. 4) for one hour to fully exhaust the LT processes without causing appreciable HT relaxation. The transition temperatures were subsequently remeasured and found to be 27.845 K and 68.51 K, respectively.

Next, both 70 K and 29 K samples were annealed at 230 K for a total time of 237 hours with numerous intermediate T_c measurements, yielding the $T_c(t)$ dependences shown in Figs. 7(a) and 7(c), respectively. The samples were then annealed at room temperature (~ 298 K) for 38 hours to exhaust any remaining relaxation, after which the transitions were again remeasured and found to be 28.55 K and 70.23 K which lie only 50 mK and 30 mK, respectively, higher than the initial values at the beginning of the first measurement series. In Figs. 6 and 7 it can be seen that the approach of

T_c to its saturation value is more gradual for the 29 K sample than for the other two, supporting our earlier observation that this sample has a larger activation energy for both LT and HT processes. To test whether the equilibrium values of T_c at ambient pressure are the same at RT and 230 K, both samples were annealed once again at 230 K for 48 hours; the transition temperatures of the 29 K and 70 K samples were observed to increase slightly by 30 mK and 50 mK, respectively [21].

Corresponding LT and HT relaxation data for the 40 K sample are shown in Figs. 6(b) and 7(b), respectively [15, 16]. The solid curves in Figs. 6 and 7 are fits to the stretched exponential expression

$$T_c(t) = T_c(\infty) - [T_c(\infty) - T_c(0)] \exp \left\{ - \left(\frac{t + t_0}{\tau} \right)^\alpha \right\}, \quad (1)$$

where $T_c(0)$ and $T_c(\infty)$ are the initial and final (fully relaxed) values of the transition temperature, respectively, τ is the relaxation time, t_0 is an additional time included to account for any relaxation that occurred before $t = 0$, and α is the stretched exponent which has been set to 0.25 for each of the plotted curve fits, as discussed below. The fit parameters are tabulated in Table 1, along with activation energies E_A calculated from the relaxation time τ using an Arrhenius law

$$\tau = \tau_0 \exp \left(\frac{E_A}{k_B T} \right), \quad (2)$$

with an attempt period $\tau_0 \simeq 10^{-12}$ seconds [22]. Note that Table 1 also includes reanalyzed curve fitting data for the 40 K sample for annealing temperatures of 225 K and 75 K.

We now describe the curve fitting procedure in more detail. For each of the fits to the HT relaxation data ($T_{anneal} = 230$ K or 225 K) the fitting process was relatively straightforward. $T_c^{RT}(0)$ was fixed to the plateau value and t_0 was set to zero under the reasonable assumption that no significant HT relaxation occurred prior to the first 230 K (or 225 K) anneal; $T_c^{RT}(\infty)$ was fixed to the value of the transition temperature following the final 38-hour room temperature anneal. Notably, all four HT data sets in Table 1 are reasonably well fit with a *single* floating parameter (the time constant τ) and a common stretch exponent $\alpha = 0.25$; smaller values of α (such as $\alpha = 0.20$) resulted in poorer fits to the 40 K data, while larger values ($\alpha = 0.30$) yielded poorer fits to the 29 K and 70 K data. The uncertainties in Table 1 in the time constants were determined by running the curve fits with maximum/minimum values of the fixed parameters and adding the associated uncertainty from the nonlinear least-squares curve fitting routine; the uncertainties in the activation energy include both the uncertainties in the time constants and the annealing temperatures.

The HT activation energy $E_A^{29K} \simeq 0.80$ eV obtained for the 29 K sample is clearly larger than for the other two samples, in agreement with the qualitative conclusions reached above from Figs. 1 and 4. Interestingly, the HT activation energy for the 40 K sample appears to be slightly smaller than that for the 70 K sample, indicating

that E_A may not change monotonically with the oxygen doping level. It is worth noting that this trend is also obtained using several other reasonable curve fitting schemes (see Ref. [23] for details).

A similar procedure was used for analyzing the LT relaxation data ($T_{anneal} = 82$ K or 75 K). For all samples, $T_c^{LT}(\infty)$ was fixed to the value of the transition temperature following annealing at the “plateau” temperature. For the 29 K sample, $T_c^{LT}(0)$ was fixed to the value of the transition temperature directly following the LT pressure release at ~ 40 K since, as seen in Fig. 4(b), the LT relaxation does not begin until higher temperatures. For the 40 K and 70 K samples, however, $T_c^{LT}(0)$ could not be directly measured in this manner because sizeable LT relaxation processes have begun at temperatures below T_c in these samples (see Figs. 1 and 4(a)). We can, however, obtain a reasonable estimate of $T_c^{LT}(0)$ in the following way. If the pressure is changed at a temperature sufficiently low to freeze out LT relaxation processes, the “non-oxygen-ordering (non-OO) derivative is given by the expression $(dT_c/dP)^{non-OO} = [T_c^{LT}(P) - T_c^{LT}(0)]/\Delta P$ for a pressure change ΔP . From this it follows that

$$T_c^{LT}(0) = T_c^{LT}(P) - \Delta P \left(\frac{dT_c}{dP} \right)^{non-OO}. \quad (3)$$

As expressed in Eq. (4) below, the change in T_c under pressure can be broken down in two components, one which excludes and the other which is determined solely by oxygen-ordering effects. Oxygen-ordering effects on T_c can be suppressed either by changing the pressure at a sufficiently low temperature, as for the strongly overdoped 29 K sample above where we find $(dT_c/dP)^{non-OO} \simeq 0$ K/GPa, or by determining dT_c/dP at any temperature on an optimally doped sample, where oxygen ordering effects, or any effect involving charge transfer, should have negligible influence on the pressure derivative [15]. For optimally doped Tl-2201, where $T_c \simeq 92$ K, it was reported previously that $dT_c/dP = (dT_c/dP)^{non-OO} \simeq +1.5 \pm 0.4$ K/GPa [5]. We now estimate $(dT_c/dP)^{non-OO}$ for samples with intermediate concentrations of interstitial oxygen by simply linearly interpolating between these two values, as shown in Fig. 8. Armed with these values of $(dT_c/dP)^{non-OO}$, we can now use Eq. (3) to estimate $T_c^{LT}(0)$, the value the transition temperature would have taken on upon release of pressure at LT had oxygen ordering effects been completely frozen out. This ad hoc method works reasonably well since for Tl-2201 the effects of oxygen-ordering on T_c dominate over the non-OO effects. For further details of the interpolation procedure, see Ref. [24].

In addition, in the fits of the relaxation data for the 40 K and 70 K samples, we include a floating parameter t_0 to account for the additional time that elapsed during the “hidden” LT relaxation. Under these constraints, reasonable fits to all four LT data sets were obtained with the same stretch exponent $\alpha = 0.25$ used for fitting the HT data.

As was the case for the HT activation energy, the LT activation energy $E_A^{29K} \simeq 0.28$ eV for the 29 K sample is clearly greater than that for the other two samples,

as concluded earlier from Figs. 1 and 4. In contrast to the HT case, however, we note that the LT activation energies are consistent with a monotonic dependence on doping level, although the difference between the 40 K and 70 K values is of marginal significance, disappearing, in fact, altogether for reasonable alternative curve fitting procedures [25].

4 Discussion

In the present experiments on Tl-2201, the application of pressure at RT may cause changes in the superconducting transition temperature T_c in at least five distinct ways: (1) the flatness of the CuO_2 plane(s) (buckling angle) increases or decreases [26], (2) hole charge carriers are transferred into the CuO_2 plane(s) even without oxygen ordering effects, (3) even at constant carrier concentration the *density* of charge carriers increases with pressure because of the decrease in the lattice parameters, (4) LT oxygen ordering effects enhance the transfer of hole charge carriers into the CuO_2 plane(s), (5) HT oxygen ordering effects enhance the transfer of hole charge carriers into the CuO_2 plane(s). Releasing the pressure at low temperatures and measuring how T_c changes as a function of the annealing temperature allows us to “see” which changes in T_c originate from LT or HT oxygen-ordering processes and which are due to other non-OO effects (i.e. pts. (1) to (3) above). The change in T_c with pressure applied at RT can thus be written as the sum of three components:

$$\left(\frac{dT_c}{dP}\right)_{RT} = \left(\frac{dT_c}{dP}\right)_{LT}^{OO} + \left(\frac{dT_c}{dP}\right)_{HT}^{OO} + \left(\frac{dT_c}{dP}\right)^{non-OO}. \quad (4)$$

The data in Figs. 3(b) and 4(b), for example, can be directly used to determine each of the above pressure derivatives for the 29 K sample. When pressure is applied at RT (Fig. 3(b)), the total change in T_c gives the first derivative $(dT_c/dP)_{RT}$. Since the LT relaxation does not begin until 69 K for the 29 K sample, releasing the pressure near 40 K freezes in completely both the LT and HT oxygen ordering effects, so that the non-oxygen-ordering derivative $(dT_c/dP)^{non-OO}$ is obtained directly from the change in T_c as pressure is released. The LT oxygen-ordering derivative is determined by the magnitude of the increase in T_c in Fig. 4(b) between 50 K and the plateau near 140 K and the HT derivative from the increase in T_c between the plateau and RT.

All data related to the pressure derivatives are summarized in Table 2 for the four oxygen concentrations considered here, plus reanalyzed results for further Tl-2201 samples published previously. For measurements in which the pressure was released at a temperature not low enough to freeze out the LT oxygen ordering processes (experiments on the 40 K, 48 K, 70 K and 83 K samples), $T_c^{LT}(0)$ has been estimated from Eq. (3), using interpolated values of $(dT_c/dP)^{non-OO}$ as described previously and as illustrated in Ref. [24]. Fig. 8 plots the various pressure derivatives in Eq. (4) versus the ambient-pressure value of T_c for Tl-2201 from the present and earlier

studies; note that in the work of Sieburger and Schilling [5] only $(dT_c/dP)_{\text{RT}}$ can be extracted. As evident from the figure, for samples with T_c between 15 K and 83 K the influence of HT processes on dT_c/dP is roughly constant (to within a factor of 2), while that of the LT process varies by more than an order of magnitude, peaking for samples with $T_c \approx 40$ K. Apparently, intermediate concentrations of excess oxygen provide more favorable conditions for the occurrence of LT ordering effects and/or their influence on T_c .

These results are perhaps best discussed in the context of the dependence of T_c on doping level n . Optimally doped $\text{Tl}_2\text{Ba}_2\text{CuO}_{6+\delta}$ samples have no excess oxygen ($\delta \simeq 0$) and exhibit transition temperatures as high as 95 K [27]; increasing δ enhances n and causes T_c to decrease in an approximately parabolic manner [28]. The steadily reduced influence of the LT ordering process as T_c increases from 40 K to 90 K is thus not surprising since T_c should become less sensitive to changes in doping level n as the optimally doped state is approached. The fact that the influence of the HT process does not undergo a similar decrease (at least not until T_c exceeds 83 K) is evidence that the strength of the HT ordering process is actually *enhanced* (or, alternately, that a given amount of ordering causes increasing amounts of doping) as the optimal doping concentration is approached; at present we have no physical explanation for how this might occur. On the other hand, the influence of both HT and LT processes on T_c decreases as T_c approaches values below 40 K, indicating that both HT and LT oxygen ordering effects cause progressively *less* change in doping level n as T_c decreases from 40 K to 0 K. This reduction in doping level must be particularly drastic, given that an increase in n should lead to a *greater* drop in T_c as the doping level proceeds further and further into the overdoped region of the T_c vs n parabola. The fact that for samples with $T_c \leq 29$ K the effects of pressure-induced oxygen ordering on T_c are so small implies either that the degree of oxygen ordering itself is diminished, perhaps because n is near a critical value n_c at which long range oxygen ordering occurs (superstructure in the oxygen defect sublattice), or oxygen ordering has minimal effect on the doping level and thus on T_c . The former scenario would seem more likely.

It would be desirable to use experimental probes on a microscopic scale (NMR) to accurately characterize the nature of the relaxation phenomena in Tl-2201 and other superconducting oxides. A comparison of these results to molecular dynamics calculations would also be of considerable interest.

Acknowledgments: This research at Washington University is supported under grant No. DMR 98-03820 by the National Science Foundation. The involvement of one of the authors (CWL) in this project was made possible by a Merrimack College Faculty Development Grant.

References

- [1] A. J. Jacobsen, J. M. Newsam, D. D. Johnston, D. P. Goshorn, J. T. Lewandowski, and M. S. Alvarez, *Phys. Rev. B* **39** (1992) 254.
- [2] Y. Shimakawa, Y. Kubo, T. Manako, H. Igarashi, F. Izumi, and H. Asano, *Phys. Rev. B* **42** (1990) 10165.
- [3] B. W. Veal, A. P. Paulikas, H. You, H. Shi, Y. Fang, and J. W. Downey, *Phys. Rev. B* **42** (1990) 6305.
- [4] B. W. Veal and A. P. Paulikas, *Physica C* **184** (1991) 321.
- [5] R. Sieburger and J. S. Schilling, *Physica C* **173** (1991) 403.
- [6] Y-123: W. H. Fietz, R. Quenzel, H. A. Ludwig, K. Grube, S. I. Schlachter, F. W. Hornung, T. Wolf, A. Erb, M. Kläser, and G. Müller-Vogt, *Physica C* **270** (1996) 258.
- [7] Y-123: S. Sadewasser, J. S. Schilling, H. Zheng, A. P. Paulikas, and B. W. Veal, *Phys. Rev. B* **56** (1997) 14168.
- [8] Y-123: S. Sadewasser, J. S. Schilling, A. P. Paulikas, and B. Veal, *Phys. Rev. B* **61** (2000) 741.
- [9] Nd-123: V. P. Dyakonov, I.M. Fita, N. A. Doroshenko, M. Baran, and H. Szymczak, *JETP Lett.* **63** (1996) 825.
- [10] Gd-123: M. Baran, V. Dyakonov, I. Fita, L. Gladczuk, A. Wisniewski, H. Szymczak, *Physica C* **267** (1996) 313.
- [11] Superoxygenated $\text{La}_2\text{CuO}_{4+\delta}$: J. E. Schirber, W. R. Bayless, F. C. Chou, D. C. Johnston, P. C. Canfield, and Z. Fisk, *Phys. Rev. B* **48** (1993) 6506.
- [12] Hg-1201: S. Sadewasser, J. S. Schilling, J. L. Wagner, O. Chmaissem, J. D. Jorgensen, D. G. Hinks, and B. Dabrowski, *Phys. Rev. B* **60** (1999) 9827.
- [13] $\text{TlSr}_2\text{CaCu}_2\text{O}_{7-y}$ (Tl-1212): C. Looney, J. S. Schilling, and Y. Shimakawa, *Physica C* **297** (1998) 239.
- [14] C. Looney, J. S. Schilling, S. Doyle, and A. M. Hermann, *Physica C* **289** (1997) 203.
- [15] A. -K. Klehe, C. Looney, J. S. Schilling, H. Takahashi, N. Mōri, Y. Shimakawa, Y. Kubo, T. Manako, S. Doyle, and A. M. Hermann, *Physica C* **257** (1996) 105.
- [16] S. Sadewasser, J. S. Schilling, and A. M. Hermann, *Phys. Rev. B* (to appear Oct. 1, 2000).

- [17] The shifts in the real and imaginary parts of the susceptibility closely paralleled each other; the real part was used in the analysis because it yielded slightly better resolution.
- [18] J. S. Schilling, J. Diederichs, S. Klotz, and R. Sieburger, in: *Magnetic Susceptibility of Superconductors and Other Spin Systems*, R. A. Hein, T. L. Francavilla, D. H. Liebenberg (Eds.) Plenum, New York, 1991, p. 107.
- [19] F. Mascarenhas, Masters Thesis, Washington University (2000).
- [20] Unfortunately, the development of a significant leak made it necessary to fully release the pressure at LT without first measuring T_c , as a substantial fraction (perhaps more than half) of the total pressure would have been lost during the 4 hours normally required to measure both transitions. The leak was negated during most of the cooldown by continuously supplying the pressure cell with high pressure helium gas from the high pressure reservoir. At 110 K, the high pressure reservoir became depleted, with the result that approximately 10% of the pressure in the cell leaked away during the 35 minutes required to cool the cell from 110 K down to 52 K. By immediately releasing the pressure at 52 K, we were able to keep the total pressure loss to an acceptable level.
- [21] Interestingly, the equilibrium T_c values for both samples *increase* (although slightly) when subjected to a higher degree of “order” (lower temperature) in annealing experiments but *decrease* when subjected to greater “order” by means of applied pressure. We have no explanation for this seemingly inconsistent behavior, although a similar anomaly has been observed in Tl-1212 (Ref. [13]). No measurable dependence of $T_c(\infty)$ on annealing temperature has been observed for the 40 K sample.
- [22] We are unaware of any measurements of τ_0 for relaxation in Tl-2201. Typical attempt periods in Y-123 range from 10^{-11} to 10^{-13} seconds: M. Weller, Mater. Sci. Forum 119-121 (1991) 667; J. R. Cost and J. T. Stanley, Scripta Metallurgica et Materialia, 28 (1993) 773.
- [23] We explored alternate HT curve fitting schemes to account for the possibility that α might vary with oxygen content or that $T_c(\infty)$ might depend significantly on annealing temperature; all reasonable schemes resulted in the non-monotonic trend described in the text. Some examples: [i] If α is allowed to float, with $T_c(0)$ and $T_c(\infty)$ fixed as described in the text, we obtain: for $\alpha = 0.21$, $E_A^{29K} = 0.807$ eV; for annealing at 230 K and $\alpha = 0.24$, $E_A^{40K} = 0.721$ eV; for annealing at 225 K and $\alpha = 0.26$, $E_A^{40K} = 0.722$ eV; for $\alpha = 0.20$, $E_A^{70K} = 0.750$ eV. [ii] If, instead, $T_c(\infty)$ is estimated using the results of the 48-hour “return anneal” at 230 K, floating α yields: for $\alpha = 0.21$, $E_A^{29K} = 0.820$ eV; for $\alpha = 0.189$, $E_A^{70K} = 0.755$ eV (the results for the 40 K sample are identical to those in case

[i]). The uncertainties in the activation energies in either case are similar to those in Table 2. [iii] Floating $T_c(\infty)$ with any reasonable value of α yields $E_A^{29K} > E_A^{70K} > E_A^{40K}$; for example, for $\alpha = 0.25$ we obtain $E_A^{29K} = 0.777$ eV, $E_A^{70K} = 0.734$ eV, and $E_A^{40K} = 0.720$ eV.

[24] For example, for the 40 K sample (75 K anneal),

$$(dT_c/dP)^{non-OO} \simeq (1.5 \text{ K/GPa}) \times [(40 \text{ K} - 29 \text{ K}) / (90 \text{ K} - 29 \text{ K})] = 0.3 \pm 0.4 \text{ K/GPa},$$

where we have assumed the interpolated pressure derivative has the same absolute uncertainty (± 0.4 K/GPa) as that reported for the 90 K sample. We then obtain

$$T_c(0) = 32.77\text{K} - (0.3 \pm 0.4 \text{ K/GPa}) \times (0.73\text{GPa}) = 32.55 \pm 0.29 \text{ K}.$$

However, $T_c(0)$ cannot be larger than the transition temperature measured (32.77 K, Ref. [15]) following the release of pressure at LT. Thus, we obtain

$$T_c(0) \simeq 32.42(15) \text{ K}.$$

Finally, we note that for the 70 K sample, we have to estimate $T_c(P)$ (from the series 1 data), which was not measured in the second data series, before estimating $T_c(0)$ from the interpolated pressure derivative.

[25] Here we qualitatively describe the results of several alternate LT curve fitting procedures. [i] As noted for the HT process in Ref. [23], floating α does not alter the trend of LT activation energies. [ii] If $T_c(0)$ is included as a *floating* parameter, the calculated 40 K and 70 K LT activation energies come out equal to each other. [iii] If we also float $T_c(\infty)$, then the LT activation energy for the 70 K sample is found to slightly exceed that of the 40 K sample. (In both [ii] and [iii], the 29 K sample continues to have the greatest activation energy.) In this connection, it is also worth noting that floating $T_c(0)$ yields $(dT_c/dP)^{non-OO}$ in the range +4 to +9 K/GPa for the 40 K crystal, which would be a very rapid rate for an overdoped sample.

[26] J. D. Jorgensen, D. G. Hinks, O. Chmaissem, D. N. Argyriou, J. F. Mitchell, and B. Dabrowski, in *Recent Developments in High Temperature Superconductivity*, edited by J. Klamut et al., Lecture Notes in Physics, Vol. 475 (Springer-Verlag, Hamburg, 1996) p. 1.

[27] H. Shaked, P. M. Keane, J. C. Rodriguez, F. F. Owen, R. L. Hitterman, and J. D. Jorgensen, *Crystal Structures of the High- T_c Superconducting Copper-Oxides*, Elsevier Science B.V. (Amsterdam) 1994, p. 9.

[28] C. Allgeier and J. S. Schilling, *Physica C* 168 (1990) 499.

[29] H. Takahashi, A.-K. Klehe, C. Looney, J.S. Schilling, N. Mōri, Y. Shimakawa, Y. Kubo, and T. Manako, *Physica C* 217 (1993) 163.

Figure Captions

Fig. 1. Results of diamond-anvil-cell experiment on Tl-2201 from Ref. [14]. Inset shows T_c as a function of pressure applied at room temperature and released at low temperature (~ 6 K). Full graph shows T_c as a function of annealing temperature following the release of pressure at 6 K. Vertical error bars are smaller than the symbols and lines are guides to the eye.

Fig. 2. The real part of the magnetic susceptibility versus temperature for Tl-2201 single crystals with $T_c(1 \text{ bar})$ near 29 K and 70 K. For both samples T_c shifts to lower temperatures under pressure.

Fig. 3. The pressure dependence of T_c for hydrostatic pressure changes at RT and LT for Tl-2201 single crystals with ambient pressure T_c values of approximately (a) 70 K and (b) 29 K. Horizontal error bars indicate pressure decrease upon cooling due to contraction of helium and a slight leak in the pressure vessel. For the 70 K sample (a), the vertical error bars are the same size as the symbols. Point #5 has been estimated from Eq. (3). Straight lines give values of dT_c/dP given in text. Numbers give order of measurements.

Fig. 4. T_c as a function of annealing temperature following the release of pressure at low temperature for Tl-2201 single crystals with ambient pressure T_c values of approximately (a) 70 K and (b) 29 K. The vertical error bars in (a) are the same size as the symbols. Solid lines are guides to the eye.

Fig. 5. T_c as a function of annealing temperature following the release of pressure at low temperature for a 15 K single crystal of Tl-2201. Inset gives dependence of T_c on pressure applied at RT (pts. 1-5) and released at LT (pt. 6). Lines are guides to the eye.

Fig. 6. T_c as a function of annealing time at 82 K for (a) 70 K, (b) 40 K (Ref. [16]), and (c) 29 K Tl-2201 crystals. The solid lines are stretched exponential fits to Eq. (1). Arrows in the right margin indicate the transition temperatures after complete relaxation. In figures (a) and (b), the uncertainties in the T_c measurements are equal to or smaller than the symbol size. Inset shows T_c vs. annealing time at 75 K for the 40 K sample (from Ref. [15]).

Fig. 7. T_c as a function of annealing time at 230 K for three (a) 70 K, (b) 40 K (Ref. [15]), and (c) 29 K Tl-2201 single crystals. The solid lines are stretched exponential fits to Eq. (1). Arrows in the right margin indicate the transition temperatures

after complete relaxation. In Figs. (a) and (b) the vertical error bars are equal to or smaller than the size of the symbols. Inset shows T_c vs. annealing time at 225 K for the 40 K sample (from Ref. [16]).

Fig. 8. dT_c/dP as a function of $T_c(1 \text{ bar})$ with and without oxygen ordering effects from present and previous studies (see legend). The solid line gives the total RT pressure derivative, whereas the dashed line represents the “non-oxygen-ordering” contribution to the pressure derivative (see Eq. (4)). The magnitudes of the HT and LT oxygen ordering contributions are represented by vertical lines and bars, respectively. The gaps and overlaps between the vertical lines and bars, which indicate slight deviations from Eq. (4), are less than the combined uncertainties in the various pressure derivatives.

Table 1: Fit parameters used for fitting the relaxation data in Figs. 6 and 7 to Eq. (1) using $\alpha = 0.25$ for all fits. Error in annealing temperature is 1% or less. See text for details of the fitting procedure.

	T_{anneal} [K]	sample	Ref.	$T_c(0)$ [K]	$T_c(\infty)$ [K]	t_0 [hours]	τ [hours]	E_A [eV]
HT	230	29 K		27.845(30)	28.55(3)		107 ⁺⁸⁹ ₋₅₁	0.803(13)
	230	40 K	[15]	38.07(3)	39.91(5)		1.9 ^{+0.6} _{-0.5}	0.723(15)
	225		[16]	38.75(5)	39.51(5)		4.1 ^{+5.4} _{-2.5}	0.722(22)
	230	70 K		68.51(5)	70.23(3)		8.8 ^{+4.0} _{-2.9}	0.753(8)
LT	82	29 K		27.445(30)	27.845(30)		76 ⁺¹⁴⁶ ₋₅₄	0.284(8)
	82	40 K	[16]	38.62(3)	38.75(5)	< 0.00002	8.3 ^{+3.6} _{-2.7}	0.268(6)
	75		[15]	32.42(15)	38.07(5)	< 0.002	85 ⁺²⁶ ₋₁₉	0.260(5)
	82	70 K		66.84(26)	68.51(5)	< 0.03	1.3 ^{+2.0} _{-0.7}	0.255(6)

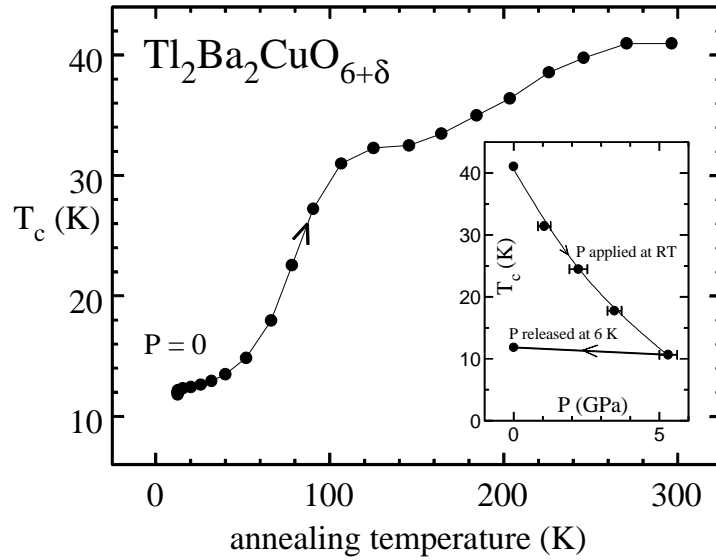


Figure 1:

Table 2: A comparison of the LT and HT relaxation data for various Tl-2201 samples following the full release of pressure at low temperature. P^{HT} and P^{LT} are the pressures to which the samples were exposed in the HT and LT oxygen ordering temperature ranges, respectively, and $P_{residual}$ is the pressure that remained following the LT pressure release. The entries at the bottom of the table, % LT and % HT, refer to the relative contributions of the LT and HT processes to the combined “oxygen ordering” pressure derivative. See text for further definitions.

sample	15 K	23 K	29 K	29 K	40 K	40 K	40 K
data source		Ref. 15	series 1	series 2	Ref. 15	Ref. 16	Fig. 1
P^{LT} [GPa]	0.59(2)	0.56(2)	0.56(5)	0.69(3)	0.76(3)	0.28(1)	5.1(3)
P^{HT} [GPa]	0.63(2)	0.61(3)	0.68(4)	0.73(1)	0.84(5)	0.31(1)	5.5(3)
$P_{residual}$ [GPa]	0	0.018	0	0	0.002	0	0
$T_c^{LT}(0)$ [K]	14.40(4)	21.07(5)	27.54(3)	27.45(3)	32.42(15)	36.62(3)	11.8(1)
$T_c(\text{plateau})$ [K]	14.84(4)	21.35(5)	27.82(3)	27.85(3)	38.07(5)	38.75(5)	32.3(7)
$T_c^{RT}(\infty)$ [K]	15.50(4)	22.40(5)	28.50(3)	28.55(3)	39.91(3)	39.51(5)	41.1(5)
ΔT_c^{LT} [K]	0.44(6)	0.28(7)	0.28(4)	0.40(4)	5.65(16)	2.13(6)	20.5(7)
ΔT_c^{HT} [K]	0.66(6)	1.05(7)	0.68(4)	0.70(4)	1.84(6)	0.76(7)	8.8(9)
$\left(\frac{dT_c}{dP}\right)_{RT} \left[\frac{\text{K}}{\text{GPa}}\right]$	-1.80(15)	-2.41(24)	-1.56(26)	—	-8.9(8)	-9.1(7)	
$\left(\frac{dT_c}{dP}\right)_{LT}^{oo} \left[\frac{\text{K}}{\text{GPa}}\right]$	+0.75(10)	+0.52(13)	+0.50(9)	+0.58(7)	+7.45(36)	+7.61(34)	+4.02(27)
$\left(\frac{dT_c}{dP}\right)_{HT}^{oo} \left[\frac{\text{K}}{\text{GPa}}\right]$	+1.05(10)	+1.77(15)	+1.00(9)	+0.97(6)	+2.20(15)	+2.45(24)	+1.60(18)
% LT	42(6)%	23(6)%	33(6)%	38(5)%	77(5)%	76(5)%	72(6)%
% HT	58(7)%	77(9)%	67(8)%	62(5)%	23(2)%	24(3)%	28(4)%

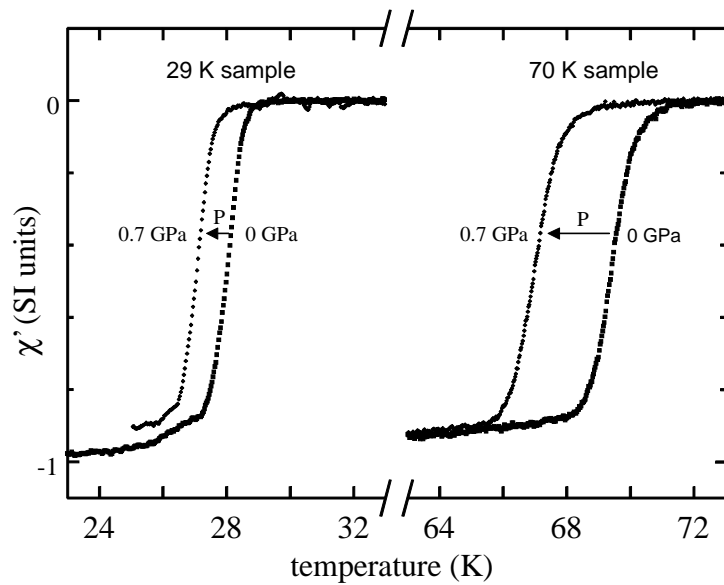


Figure 2:

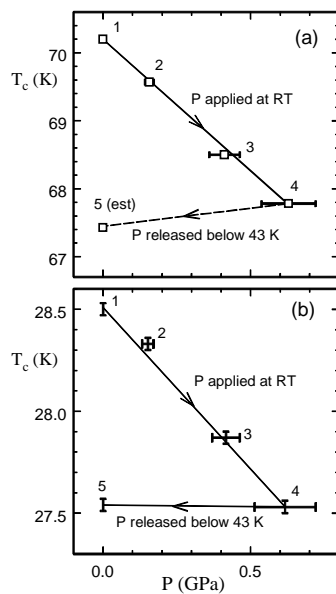


Figure 3:

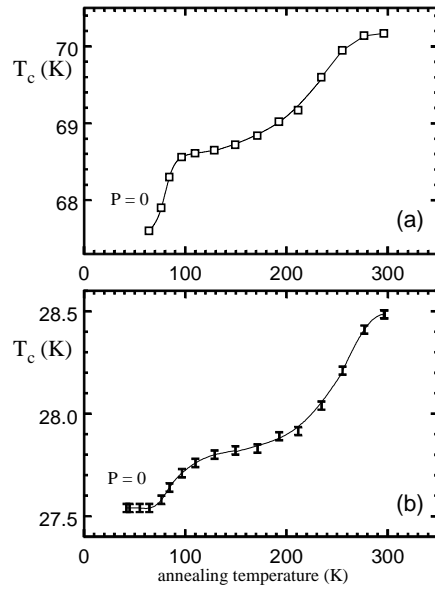


Figure 4:

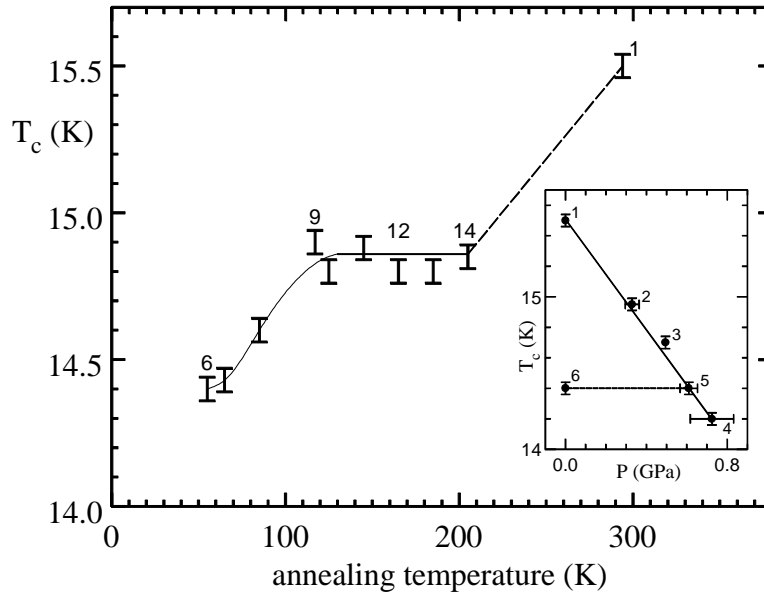


Figure 5:

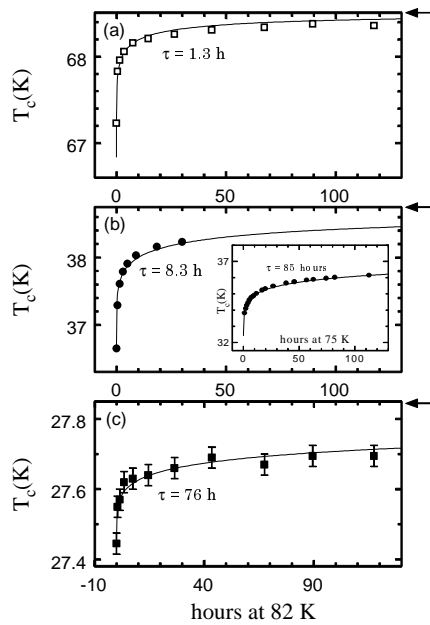


Figure 6:

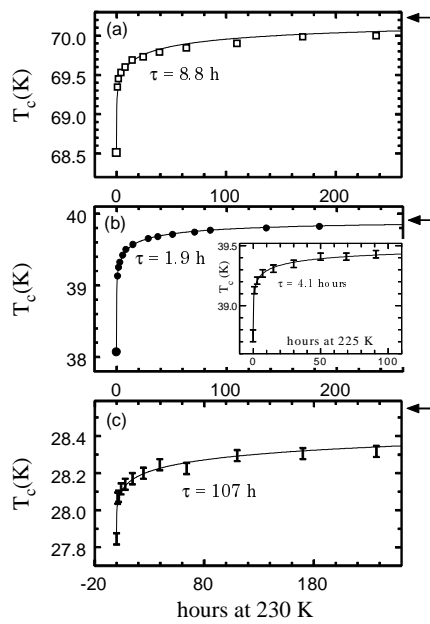


Figure 7:

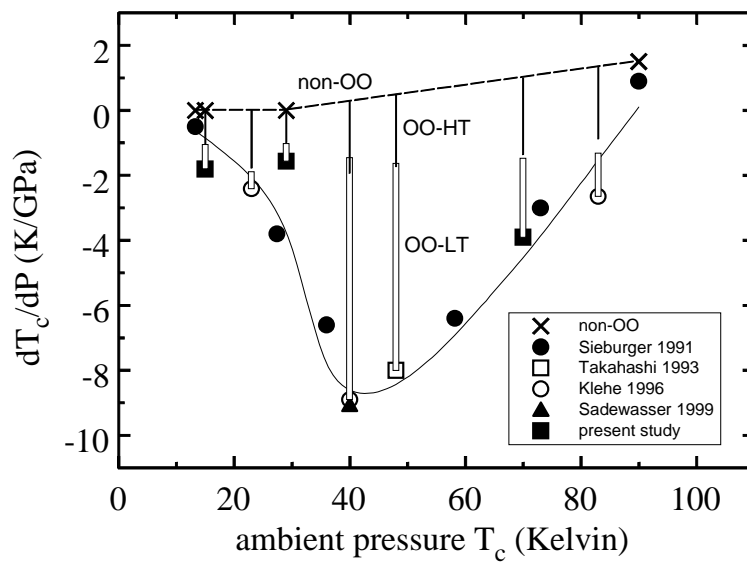


Figure 8: